

Fourier Transform Ion Mobility Measurement of Chain Branching in Mass-Selected, Chemically Trapped Oligomers from Methylalumoxane-Activated, Metallocene-Catalyzed Polymerization of Ethylene

Rolf Dietiker, Fabio di Lena, and Peter Chen*

Contribution from the Laboratorium für Organische Chemie, ETH Zürich, Switzerland

Received July 29, 2006; E-mail: peter.chen@org.chem.ethz.ch

Abstract: Fourier transform ion mobility spectrometry is used to determine the branching in mass-selected, chemically trapped oligomers produced in the polymerization of ethylene by a metallocene catalyst activated by methylalumoxane. The measured branching is included in a kinetic analysis to extract the activation energies for the elementary steps in polyethylene formation. Propagation, chain transfer, and chain walking have activation energies of 4.1, 11, and 11 kcal/mol.

Introduction

The assessment of catalyst performance or material properties in polymer chemistry presents technical challenges which have been increasingly addressed by various forms of physical measurement. Polymer analysis, in particular, is complicated by the polydispersity of the material itself. Polymer samples are ensembles of closely related molecules which are often difficult to separate and nearly impossible to characterize within the mixture. The polymerization process is usually studied by examining the macroscopic kinetics,¹ but there can be difficulties associated with this procedure. We recently reported a kinetic approach to Ziegler–Natta polymerization of olefins based on trapping of the intermediate chains and detection of the metal-bound oligomers, or their trapped products, and subsequent analysis by means of electrospray ionization tandem mass spectrometry.^{2,3} Pseudo-first-order rates for elementary reactions are entered as fit parameters into a set of coupled differential equations describing the polymerization process and then varied to reproduce experimentally observed oligomer distributions in short-time quenched polymerizations. The kinetic method extracts the elementary initiation, propagation, and chain-transfer rate constants and moreover their temperature dependences, which, when reinserted into the rate expressions, reproduces the molecular weight distribution of polymer synthesized under conditions other than those under which the kinetic measurements were done, even though original polymerization itself was interrupted at a very early stage. While the polymer molecular weight distribution is one of the decisive metrics for materials properties, it is not the only one. The extent of chain branching, for which several possible mechanisms exist, is a further, major determinant of bulk polymer properties for which

experimental techniques are less extensive. GPC with carefully calibrated reference polymers and ¹³C NMR are the usual methods, but they produce only a branching index for the entire ensemble of oligomers and polymers. Given that the kinetic modeling of a polymerization process at the level of elementary processes requires a measure of the chain branching as a function of chain length, new methodology is needed. We propose here the application of high-resolution, Fourier transform ion mobility spectrometry (FT-IMS) as a solution to the size-selected determination of chain branching in methylalumoxane (MAO)-activated, metallocene-catalyzed Ziegler–Natta polymerization.⁴ While the present study shows overall plausibility of the method and furthermore yields activation energies for key reactions, including the branching process, the ultimate product of the line of research is a predictive kinetic model for Ziegler–Natta polymerization usable in the rational optimization of catalyst structure and process conditions.

Experimental Section

The design was adapted from that of Hill⁵ and required modifications in the Finnigan MAT TSQ-700 mass spectrometer, chief among which was the addition of cooling for the electrospray ionization (ESI) source itself. A schematic diagram of the ion mobility stage added between the ESI source and the heated capillary is shown in Figure 1. The ions produced in the ESI source are injected into the countercurrent, atmospheric pressure N₂ flow (800–1000 mL/min N₂ flow rate with N₂ at 180 °C to facilitate desolvation) and fall through a potential of 5–6 kV before entering the mass spectrometer itself. The drift tube is equipped with two Bradbury–Nielsen gates separated by 12 cm. The gates are driven with a square wave potential (45–50 V pp) with frequency from a few hertz to a few kilohertz. The convolution of the two square waves on the gates is a sawtooth transmission function for the drift tube as a whole. A sweep of the frequency of this sawtooth

(1) Schnell, D.; Fink, G. *Angew. Makromol. Chem.* **1974**, *39*, 131. Fink, G.; Zoller, W. *Angew. Makromol. Chem.* **1981**, *182*, 3265. Fink, G.; Schnell, D. *Angew. Makromol. Chem.* **1982**, *105*, 31. Mynott, R.; Fink, G.; Fenzl, W. *Angew. Makromol. Chem.* **1987**, *154*, 1.
(2) Hinderling, C.; Chen, P. *Angew. Chem., Int. Ed.* **1999**, *38*, 2253.
(3) DiLena, F.; Quintanilla, E.; Chen, P. *Chem. Commun.* **2005**, 5757.

(4) Kaminsky, W.; Miri, M.; Sinn, H. J.; Woldt, R. *Makromol. Chem. Rapid Commun.* **1983**, *4*, 417.
(5) Knorr, F. J.; Eatherton, R. L.; Siems, W. F.; Hill, H. H. *Anal. Chem.* **1985**, *57*, 402. Wu, C.; Siemens, W. F.; Asbury, G. R.; Hill, H. H. *Anal. Chem.* **1998**, *70*, 4929.

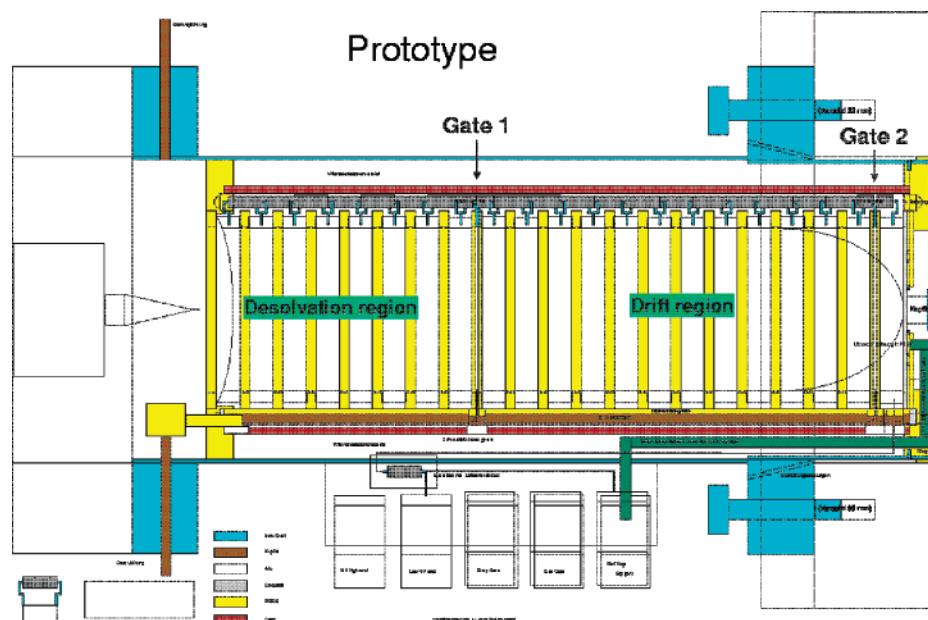


Figure 1. Schematic of the Fourier transform ion mobility stage built between the electrospray source and the Finnigan-MAT TSQ-700 triple-quadrupole mass spectrometer.

produces for a single species a sinusoidal modulation of the ion current, which upon Fourier transform recovers the mobility spectrum. To correlate the structure of the metal-bound oligomers, trapped in situ with *N,N'*-dicyclohexylcarbodiimide (DCC; and an electrophilic covalent trap), with the ion mobility, reference structures with well-defined molecular weight and chain branching were prepared by reaction of the appropriate Grignard reagent with DCC, followed by protic workup. As representative structures, the trapping products corresponding to four of the C_5 chains and two of the C_7 chains were synthesized.

The geometries of the amidinium cations derived from six C_5 chains, eighteen C_6 amidiniums, and five C_7 chains were computed with PM3. Most of the structures were also optimized at the B3LYP/6-31G level with Gaussian 03⁶ on a Linux workstation cluster. Unsurprisingly, the two quantum mechanical methods gave very similar geometries. Collision cross-sections or, equivalently, ion mobilities for all of the computed structures were computed with MOBICAL, made available as a source code or Windows executable by Jarrold and co-workers.⁷ Computational studies were conducted on DCC-trapped C_5 chains (6 compounds), shown in Figure 3, C_6 chains (18 compounds), shown in Figure 4, and C_7 chains (5 compounds), shown in Figure 5, using three different physical models for ion mobility.

To demonstrate the plausibility of the ion mobility as a means to measure chain walking rates, data were taken for samples produced in a limited number of well-characterized polymerization runs as reported in our previous paper.³ A toluene solution of Cp_2ZrCl_2 (4 mg, 13.7 μ mol) was activated by adding 100 μ L of MAO in toluene (Aldrich, 10% (w/w) solution in toluene, 165 μ mol) in a tubular glass pressure reactor (20×2.5 cm)⁸ to make a total liquid volume of 6.0 mL. The reactor was designed to circumvent the technical problems in performing kinetics on highly active polyolefin catalysts outlined by Busico.⁹ The reaction was kept saturated with ethylene at a constant total pressure

of 2.0 bar (MKS Baratron capacitance manometer) and held at 0, 60, or 120 $^{\circ}C$ in a constant-temperature bath. The solution was stirred magnetically at 1000–1500 rpm with a 4 cm stirring bar oriented vertically and undergoing precessional motion, which has the effect of moving the reaction solution up the walls of the reactor in a rapidly moving, thin annulus of liquid. The arrangement served to improve both heat and mass transport and is a prerequisite for reliable kinetic measurements. The reaction was quenched after a short time interval, usually either 300 or 90 s, by rapid injection of 35 equiv, relative to the metallocene, of DCC. Two drops of the quenched solution were diluted in 30 mL of CH_2Cl_2 and electrosprayed. The quench time was set early enough so that neither precipitation of polymer nor a significant increase in viscosity appears. Moreover, variation of the time interval separating addition of DCC and dilution and analysis from 1 to 30 min produced no discernible change in the mass spectrum, indicating that quenching was complete even at the shortest times. Subsequent addition of excess Brønsted acid did not affect the intensities of the amidinium cations in the ESI-MS. The procedure and conditions for analysis by electrospray ionization mass spectrometry have been previously described in our work on ethylene polymerization by the much less problematic late-transition-metal catalysts.¹⁰ The odd and even oligomer chain distributions, described in that earlier work, and observed here as a series of amidinium cations, were fit to a modified Cossee–Arlmann mechanism¹¹ for Ziegler–Natta polymerization, implemented as a set of coupled differential equations in PowerSim 2.5c.¹² The equations were integrated numerically and fit to the experimental distributions by means of a genetic algorithm in which the elementary rates enter as variable optimization parameters. The amidinium cations show excellent detection characteristics in ESI-MS. For the purpose of method development, the sampled distributions of amidinium cations with different lengths and differently branched alkyl chains were deemed sufficient. It should be noted that analysis of the short-time quenched oligomer distributions successfully predicted the final molecular weight of the polymer in the earlier case with palladium catalysts¹⁰ and that the measurements gave quantitatively reproducible results in a different laboratory.¹³

(6) Frisch, M. J.; et al. *Gaussian 03*, revision C.02; Gaussian, Inc.: Wallingford, CT, 2004.

(7) Mesleh, M. F.; Hunter, J. M.; Shvartsburg, A. A.; Schatz, G. C.; Jarrold, M. F. *J. Phys. Chem.* **1996**, *100*, 16082. Shvartsburg, A. A.; Jarrold, M. F. *Chem. Phys. Lett.* **1996**, *86*, 261. Mesleh, M. F.; Hunter, J. M.; Shvartsburg, A. A.; Schatz, G. C.; Jarrold, M. F. MOBICAL, <http://nano.chem.indiana.edu/Software/mobcal.tar.gz>, 1996.

(8) The reactor is the same as used in our earlier studies on catalytic hydrogenation, which shares the problems of heat and mass transport. Hartmann, R.; Chen, P. *Adv. Synth. Catal.* **2003**, *345*, 1353.

(9) Busico, V.; Cipullo, R.; Cutillo, F.; Vacatello, M. *Macromolecules* **2002**, *35*, 349.

(10) Hinderling, C.; Chen, P. *Int. J. Mass Spectrom. Ion Processes* **2000**, *195/196*, 377.

(11) Cossee, P. *Tetrahedron Lett.* **1960**, *1* (38), 12.

(12) Powersim A.S., P.O. Box 206, N-5100 Isdalstø, Norway.

(13) Santos, L. S.; Metzger, J. O. *Angew. Chem., Int. Ed.* **2006**, *45*, 977.

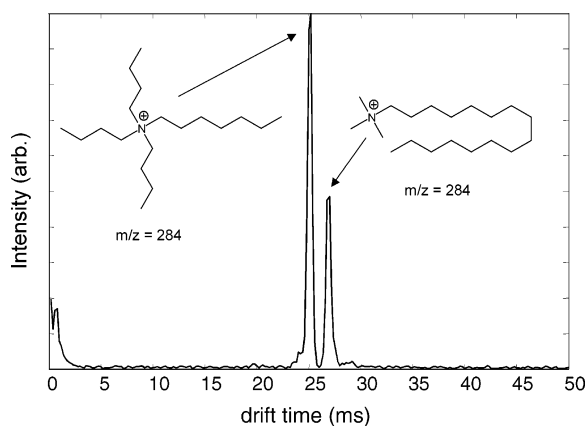
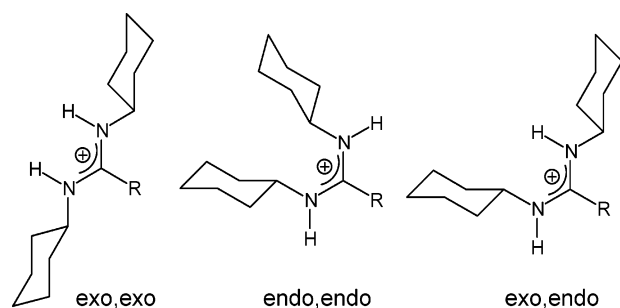


Figure 2. Mass-selected FT mobility spectrum of two electro sprayed quaternary ammonium salts, showing clean baseline separation of the isomeric ions.

Scheme 1



Results

Control studies and validation of the FT ion mobility stage in the triple-quadrupole mass spectrometer were done for representative isomeric ions before actual data for oligomer samples were taken. Isomeric quaternary ammonium cations were baseline separated, as seen in Figure 2. Moreover, protonated phthalic and terephthalic acid cations could also be cleanly distinguished. While the differences between the two quaternary ammonium salts, or phthalic versus terephthalic acid, may be expected to be large, one might wonder whether the subtle differences between the various branched amidinium cations would be detectable. Relative cross-sections differing by 6% are resolvable to baseline in the FT mobility spectrum. Even smaller differences of $\sim 2\%$ can be reliably resolved.

Interestingly, experimental investigation of the amidinium cations produced from DCC quenching of Grignard reagents revealed that they had a mobility different from that of amidinium cations produced from quenching and workup of alkylmetalloceniums. We attribute the difference in mobility to different configurations, e.g., *exo,exo* versus *exo,endo* versus *endo,endo* (Scheme 1), which can appear even for cases where the alkyl chain, R, is the same. Equilibration of the amidines in CH_3OH for a few minutes at room temperature brought all of the amidines with a given alkyl chain (length and branching) to the same structure, as could be monitored by changes in the mobility spectrum of the C_5 reference chains. It is not clear why the amidinium cations produced from the trapped alkylmetallocenium cations should be different from those produced by the synthesis via Grignard reagents, but equilibration in methanol produces the most stable isomer, regardless of the source of the molecule, which is presumed to be the *exo,exo*

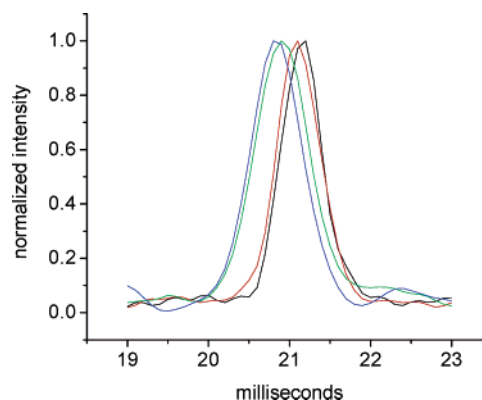


Figure 3. Mass-selected FT mobility spectrum of four methanol-equilibrated amidinium cations prepared from structurally well-defined Grignard reagents. The four isomeric C_5 alkyl chains, 1-pentyl (black), 2-pentyl (red), 2-methyl-2-butyl (green), and 2-methyl-1-butyl (blue), differ by the amount and position of branching.

isomer on the basis of calculations (PM3, DFT) on the three amidinium cations with $\text{R} = n\text{-propyl}$. One could speculate that methanol selectively stabilizes the *exo,exo* isomer by virtue of better hydrogen bonding. Last, methanol equilibration shifts the ion mobility to lower drift times (higher mobility, lower cross-section) in the control experiment. The mobility spectra, normalized to the same intensity, of several methanol-equilibrated, Grignard-derived amidiniums with predefined C_5 reference chains are shown overlaid in Figure 3. Although the peaks overlap, the differences are real and reproducible. The peaks are slightly asymmetric with a broadened base relative to a Gaussian. This peak shape has been discussed previously by Hill and can be attributed to the Fourier transform of an interferogram produced with a sawtooth transmission function.¹⁴ The maximum of the peak can be extracted by a fit to up to three Gaussians, which can distinguish between species whose cross-section differs by 0.5% when the data are of sufficient quality for a good fit.

An examination of Figure 4 shows that, for the DCC-quenched unbranched C_5 chain, the *exo,exo* and *endo,endo* isomers are computed to have similar cross-sections (within 1% of each other), both of which are significantly smaller than that for the *exo,endo* isomer. Accordingly, the computational and experimental results indicate that the methanol-equilibrated ion is very likely the *exo,exo* isomer. Given that the quenching of the Ziegler–Natta polymerization was followed by a methanolic workup, subsequent analysis assumes the *exo,exo* structure for the amidiniums. As is evident from all of the computational results and the experimental spot-checks, Figures 4–6, the branched oligomers show higher mobility than the linear isomers, regardless of the extent and type of branching. This is the principal basis on which the experimental design for determination of branching parameters in the kinetic model will be based. Having computed the cross-sections of the reference amidinium cations and checked them against representative model compounds synthesized independently, samples of DCC-quenched oligomers from MAO-activated, Cp_2ZrCl_2 -catalyzed Ziegler–Natta polymerization of ethylene were analyzed by the FT ion mobility. Representative mobility spectra are shown in Figure 7 for a mass-selected C_6 amidinium cation produced at

(14) St. Louis, R. H.; Siems, W. F.; Hill, H. H. *Anal. Chem.* **1992**, *64*, 171. Chen, Y. H.; Siems, W. F.; Hill, H. H. *Anal. Chim. Acta* **1996**, *334*, 75.

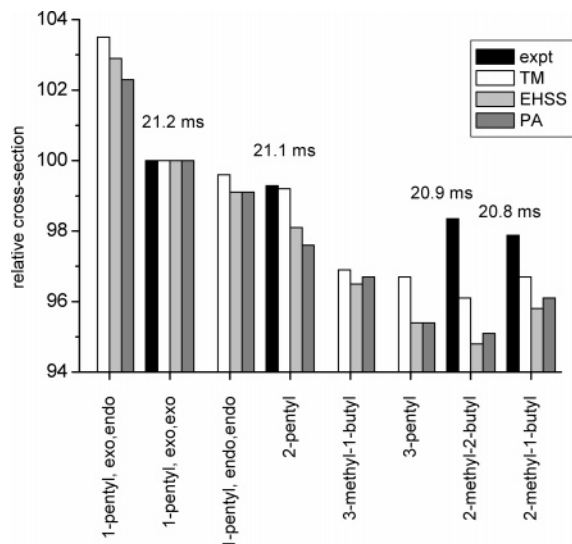


Figure 4. Comparison of the computed and measured (normalized) cross-sections for DCC-trapped, isomeric C_5 chains. The cross-sections were computed using three different methods. The three amidinium isomers are shown for the unbranched chain. For the branched chains, the computed values are for the *exo,exo* isomer. The experimental drift times, ms, are indicated for four of the isomers. Note that the vertical scale has been truncated to magnify the differences in mobility.

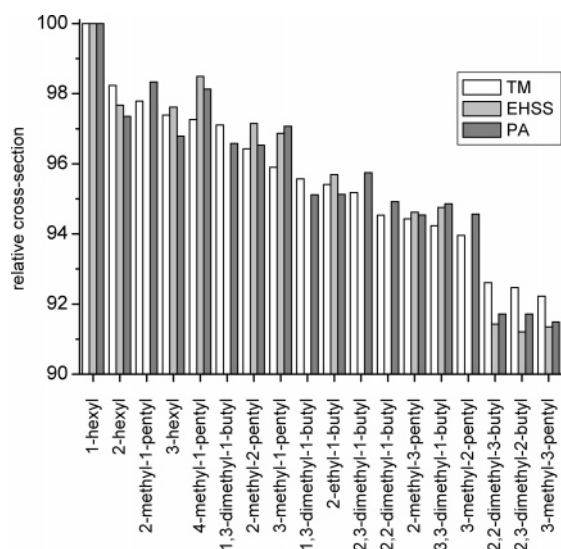


Figure 5. Comparison of the computed (normalized) cross-sections for DCC-trapped, isomeric C_6 chains. The cross-sections were computed using three different methods. All of the amidinium ions were computed as the *exo,exo* isomers. Note that the vertical scale has been truncated to magnify the differences in mobility.

two different polymerization temperatures. A complete mass spectrum, with fit, is shown in Figure 8. The extent of branching is known to increase with the polymerization temperature, and the observed differences in the ion mobility spectrum for the different temperatures are reproducible, so given the computations and control experiments, it is reasonable to attribute the higher mobility components to branched structures. The relative amounts of unbranched versus branched amidinium cations for a given mass can be extracted by deconvoluting the somewhat overlapping peaks using one or more Gaussians for the main peak (the unbranched isomer) and one or two Gaussians for the overlapping peaks due to the branched isomers. The results

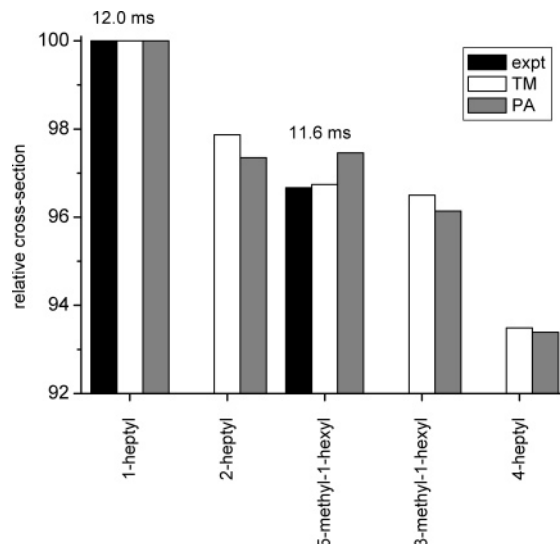


Figure 6. Comparison of the computed and measured (normalized) cross-sections for DCC-trapped, isomeric C_7 chains. The cross-sections were computed using two different methods. All of the amidinium ions were computed as the *exo,exo* isomers. The experimental drift times, in ms, are indicated for two of the isomers. Note that the vertical scale has been truncated to magnify the differences in mobility.

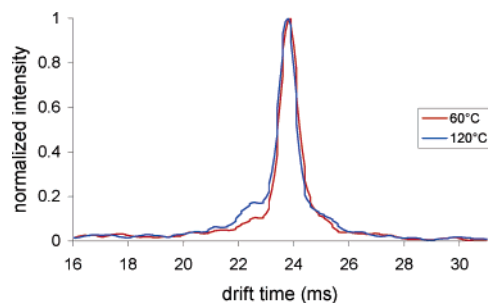


Figure 7. Comparison of the mobility spectra for mass-selected, DCC-trapped, isomeric C_6 chains from an MAO-activated, metallocene-catalyzed Ziegler–Natta polymerization at two temperatures. The experimental drift times, in ms, are indicated. The main peak is due to the linear chains. The higher temperature polymerization shows a partially resolved peak at higher mobility which is assigned to branched isomers.

of the deconvolution are shown for DCC-quenched C_5 and C_6 chains at three different temperatures in Table 1.

Discussion

Of the many factors influencing the bulk properties of a polymer,¹⁵ the most commonly cited are the molecular weight and the polydispersity. More recently, the importance of the microstructure has been increasingly recognized, with the extent and type of branching in polyolefins now being recognized as playing decisive roles in the glass temperature, melting temperature, rheological properties, and crystallinity.^{16–19} Chain walking has even been exploited as a deliberate strategy to produce highly branched polyethylene with specific properties.²⁰ Existing physical methods for measuring branching assay the

- (15) Tuchbreiter, A.; Mülhaupt, R. *Macromol. Symp.* **2001**, *173*, 1.
- (16) Suhm, J.; Heinemann, J.; Thomann, Y.; Thomann, R.; Maier, R.-D.; Schleis, T.; Okuda, J.; Kressler, J.; Mülhaupt, R. *J. Mater. Chem.* **1998**, *8*, 553.
- (17) Mäder, D.; Heinemann, J.; Walter, P.; Mülhaupt, R. *Macromolecules* **2000**, *33*, 1254.
- (18) Chum, P. S.; Kruper, W. J.; Guest, M. J. *Adv. Mater.* **2000**, *12*, 1759.
- (19) Malmberg, A.; Kokko, E.; Lehmus, P.; Löfgren, B.; Seppälä, J. V. *Macromolecules* **1998**, *31*, 8448.
- (20) Guan, Z.; Cotts, P. M.; McCord, E. F.; McLain, S. J. *Science* **1999**, *283*, 2059.

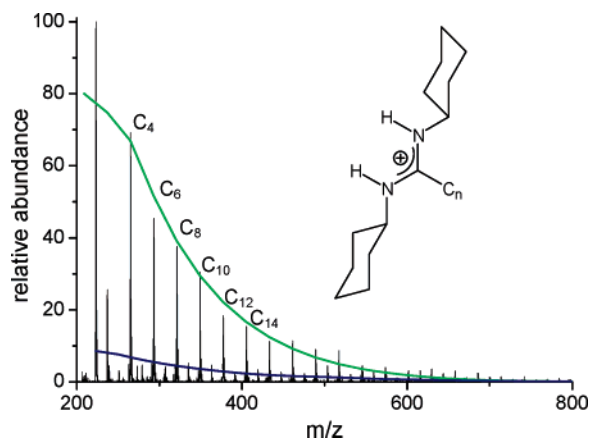


Figure 8. Electrospray ionization mass spectrum of the MAO-activated, Cp_2ZrCl_2 -catalyzed polymerization of ethylene at 120 °C, quenched after 90 s with DCC, worked up, and sprayed from methanol. Fits to the kinetic scheme depicted in Scheme 2 produce pseudo-first-order rates for initiation, propagation, chain transfer, and chain walking. The fits to the odd distribution (centers that have never undergone chain transfer) and the even distribution (centers that have undergone chain transfer at least once) are superimposed on the distributions in blue and green, respectively.

Table 1. Measured Extent of Branching in Mass-Selected, DCC-Quenched Oligomer Chains Produced by MAO-Activated, Metallocene-Catalyzed Ziegler–Natta Polymerization of Ethylene

reaction temp (°C)	DCC-quenched oligomer	% branched chains (exptl)	% branched chains (kinetic model)
0	C ₅	<2	<1.4
60	C ₅	8.5	9.2
60	C ₆	7.3	6.9
120	C ₆	23	23

bulk polymer, which provides only a slim experimental basis for the parametrization of microscopic kinetic models that are beginning to provide predictive guidance to process control and design.^{21,22} The microscopic kinetic models work by direct numerical integration of the (usually) nonlinear differential equations representing elementary processes in the polymerization reaction, for which rates or rate constants must somehow be obtained. Rytter has discussed the difficulties of using rates derived from batch experiments, which, of necessity, represent time averages over the entire reaction and which are generally poorly suited for use in microscopic models.²³ Our previous work concentrated on determining the pseudo-first-order rates, and consequently rate constants, for initiation, propagation, and chain transfer at defined time points for kinetic modeling. The present work is motivated largely by the desire to develop a method for assaying branching at a defined time point for a given oligomer selected according to molecular weight from within an ensemble of oligomers. The chosen method, ion mobility, has been implemented in a variety of applications,^{24,25} including the conformations of biomolecules²⁶ and semiconductor clusters,²⁷ and conformational studies on synthetic poly-

mers,²⁸ but not for branching in Ziegler–Natta polymerization, especially with mass selection. Isomeric peptides, differing from each other in their sequence, but not their composition, have been separated by ESI-IMS.²⁹ Significantly, ion mobility has been used to distinguish between configurational isomers produced in the early stages of polymerization,³⁰ which suggests that the present application may be reasonable. The feasibility of such a study requires better resolution than is usually afforded in ion mobility spectrometers. The introduction of FT-IMS by Hill⁵ potentially provides a method of sufficient resolution.

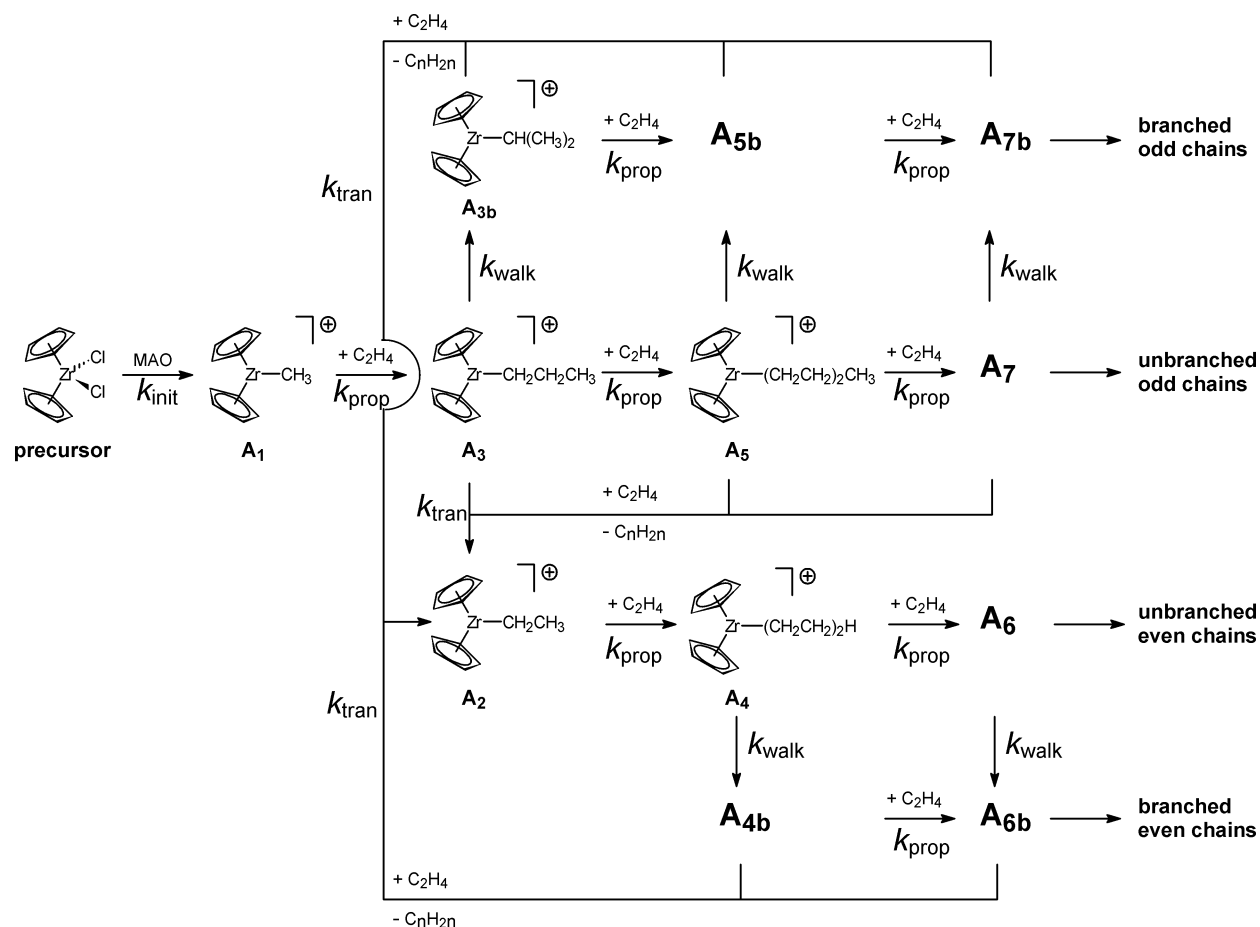
Several, increasingly sophisticated, physical models were implemented within MOBCAL and tested against selected, structurally defined ions to test whether it would be likely that FT-IMS can distinguish between linear and branched polyolefin chains. The three physical models in this study that convert molecular structures to cross-sections are the projection approximation (PA),³¹ exact hard sphere scattering (EHSS),³² and the trajectory method (TM).³³ The PA and EHSS methods model the molecule as a collection of overlapping hard spheres with radii equal to hard sphere collision distances. The PA method defines the cross-section as the integral of the summed cross-sections of the collection of hard spheres over all possible directions. In the EHSS method, the orientationally averaged momentum-transfer cross-section is calculated by determining the scattering angles between the incoming and outgoing trajectories of a buffer gas atom on the hard sphere model surface. The more sophisticated TM calculation treats the ion as a collection of atoms, each represented by a 12–6–4 potential. An effective potential obtained by summing over the individual atomic contributions is then used for classical trajectories from which one obtains the scattering angles, and ultimately, the cross-section. Although TM calculations require a large number of trajectories, typically 10^5 – 10^7 , to achieve statistically significant results, the method treats ion–molecule interactions well enough that it usually suffices as a predictor of drift times in ion mobility experiments. More sophisticated methods, e.g., scattering on electron density isosurfaces (SEDIs) or isodensity trajectory hybrid methods (SEDI-TC), incorporate inhomogeneous repulsive interactions and molecular orbital mixing effects, but their predictions and those of the simpler TM method approach each other as the ions get larger.³⁴ Accordingly, the PA, EHSS, and TM methods were checked in this study.

Even a cursory comparison of the computed relative cross-sections to the experimental spot-checks shows that the TM method produces, as expected, the best predictions for the amidinium cations produced by DCC quenching of the polym-

- (21) Wang, W. J.; Yan, D.; Zhu, S.; Hamielec, A. E. *Macromolecules* **1998**, *31*, 8677. Beigzadeh, D.; Soares, J. B. P.; Hamielec, A. E. *J. Appl. Polym. Sci.* **1999**, *71*, 1753.
 (22) Lo, D. P.; Ray, W. H. *Ind. Eng. Chem. Res.* **2005**, *44*, 5932.
 (23) Thorshaug, K.; Støvneng, J. A.; Rytter, E.; Ystenes, M. *Macromolecules* **1998**, *31*, 7149.
 (24) Clemmer, D. E.; Jarrold, M. F. *J. Mass Spectrom.* **1997**, *32*, 577.
 (25) Wyttenbach, T.; Bowers, M. T. *Top. Curr. Chem.* **2003**, *225*, 207. Wyttenbach, T.; Baker, E. S.; Bernstein, S. L.; Ferzoco, A.; Gidden, J.; Liu, D.; Bowers, M. T. *Adv. Mass Spectrom.* **2004**, *16*, 189.
 (26) Hudgins, R. R.; Woenckhaus, J.; Jarrold, M. F. *Int. J. Mass Spectrom.* **1997**, *165*, 497.

- (27) Shvartsburg, A. A.; Hudgins, R. R.; Dugourd, P.; Jarrold, M. F. *Chem. Soc. Rev.* **2001**, *30*, 26.
 (28) Gidden, J.; Kemper, P. R.; Shammel, E.; Fee, D. P.; Anderson, S.; Bowers, M. T. *Int. J. Mass Spectrom.* **2003**, *222*, 63 and references therein.
 (29) Wu, C.; Siems, W. F.; Klasmeyer, J.; Hill, H. H. *Anal. Chem.* **2000**, *72*, 391.
 (30) Alsharaeh, E. H.; Ibrahim, Y. M.; El-Shall, M. S. *J. Am. Chem. Soc.* **2005**, *127*, 6164. Momoh, P. O.; Abrash, S. A.; Mabrouki, R.; El-Shall, M. S. *J. Am. Chem. Soc.* **2006**, *128*, 12408.
 (31) von Helden, G.; Hsu, M. T.; Gotts, N. G.; Bowers, M. T. *J. Phys. Chem.* **1993**, *97*, 8182. von Helden, G.; Hsu, M. T.; Gotts, N. G.; Kemper, P. R.; Bowers, M. T. *Chem. Phys. Lett.* **1993**, *204*, 15.
 (32) Shvartsburg, A. A.; Jarrold, M. F. *Chem. Phys. Lett.* **1996**, *86*, 261.
 (33) Mesleh, M. F.; Hunter, J. M.; Shvartsburg, A. A.; Schatz, G. C.; Jarrold, M. F. *J. Phys. Chem.* **1996**, *100*, 16082. Mesleh, M. F.; Hunter, J. M.; Shvartsburg, A. A.; Schatz, G. C.; Jarrold, M. F. *J. Phys. Chem. A* **1997**, *101*, 968.
 (34) Shvartsburg, A. A.; Liu, B.; Jarrold, M. F.; Ho, K. M. *J. Chem. Phys.* **2000**, *112*, 4517.

Scheme 2



erization reactions. Consulting the MOBCAL calculations, it is evident that the linear chain amidinium cation always has the lowest mobility for all chain lengths, regardless of the physical model used for the calculation of the cross-section. The proposition that all branched-chain amidines show a lower cross-section, and hence higher mobility, compared to the unbranched isomer is furthermore borne out by spot-checks on independently synthesized model compounds. Even one branch increases the mobility by several percent, and the effect seems to be larger for the longer chains. Given that differences of $\sim 2\%$ are resolvable in the spectrometer, and differences of 0.5% can be deconvoluted, branched and unbranched chains can be distinguished, but not different degrees or locations of branching. This level of resolution leads directly to a reduced kinetic model for Ziegler-Natta polymerization, including chain walking. The model is based on the Cossee-Arlman mechanism,¹¹ which is generally accepted for metallocene-catalyzed polymerizations.

The reduced kinetic model for Ziegler-Natta polymerization is represented in Scheme 2. It resembles the stochastic model for branched polyethylene formation reported by Ziegler and co-workers.³⁵ In that work, relative rates for the different steps were obtained computationally by DFT and then used in a forward simulation of the overall branching index of polymer produced by polymerization of ethylene with late-transition-metal catalysts. In contrast to Ziegler's work, where the rates were entered as fixed parameters, the rates for initiation, chain

propagation, chain transfer, and chain walking are treated in the present model as fit parameters independent of the chain length and extracted from experimental distributions. The assumption that the rates are independent of the chain length should be acceptable once the chain length exceeds three carbons. More contentious is the assumption that the rates are largely independent of branching. Supporting the assumption is the observation by Busico³⁶ that, while subsequent insertion of another propylene after a 2,1-(mis)insertion of propylene in a metallocene catalyst is slowed 100–1000-fold, insertion of an ethylene unit subsequent to propylene is largely independent of whether the propylene inserted 1,2 or 2,1. Consequently, it should be reasonable in the present reduced kinetic model to assume a uniform propagation rate constant (for ethylene insertion) for catalyst centers carrying both branched and unbranched chains. A more refined model to account for any remaining difference would require a greatly expanded data set. The limited set of samples was used because pseudo-first-order rates for initiation, propagation, and associative chain transfer had already been extracted for a body of samples with the reduced model for which the polymerization conditions were well-characterized and well-controlled. Within Scheme 2, the branching data in Table 1 should then produce pseudo-first-order chain-walking rates for three temperatures, which is the minimum needed for an Arrhenius analysis. The object, the

(35) Michalak, A.; Ziegler, T. *J. Am. Chem. Soc.* **2002**, *124*, 7519. Michalak, A.; Ziegler, T. *Macromolecules* **2003**, *36*, 928.

(36) Busico, V.; Cipullo, R.; Talarico, G.; Caporaso, L. *Macromolecules* **1998**, *31*, 2387. Busico, V.; Cipullo, R.; Ronca, S. *Macromolecules* **2002**, *35*, 1537.

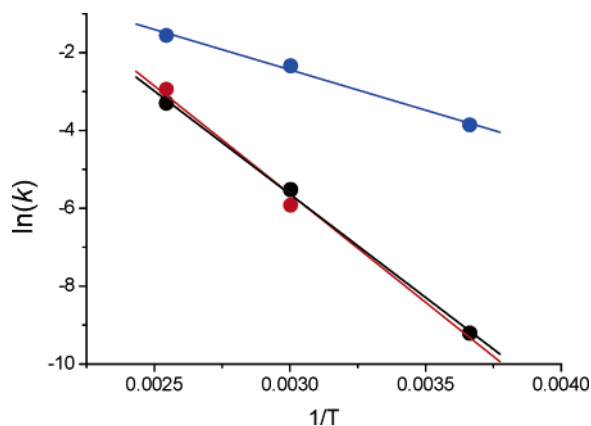


Figure 9. Arrhenius plots of the temperature-dependent pseudo-first-order rates for propagation (blue), chain transfer (red), and chain walking (black) in MAO-activated, Cp_2ZrCl_2 -catalyzed polymerization of ethylene.

activation energy for chain walking, is a quantity that can be compared to computational results.

Numerical integration of Scheme 2, with variation of k_{init} , k_{prop} , k_{trans} , and k_{walk} , produces the pseudo-first-order rates for initiation, propagation, (associative) chain transfer, and chain walking. Initiation showed non-Arrhenius behavior, but the three more relevant kinetic phenomena produced the Arrhenius plots shown in Figure 9, from whose slopes one derives the activation energies for the three kinetic events. The apparent non-Arrhenius behavior in the initiation step could be a consequence of the reduced kinetic model in which the several steps of methylation and ionization are treated as a single kinetic event. Alternatively, it could be due to relative insensitivity of the fit to variations in the initiation rate for the higher temperature data sets. In any case, the data do not allow a distinction between these alternatives at present.

With the caveat that the numerical results depend on the adequacy of the minimalistic model, one obtains $E_{\text{a,prop}} = 4.1$ kcal/mol, $E_{\text{a,trans}} = 11$ kcal/mol, and $E_{\text{a,walk}} = 11$ kcal/mol. Comparison to activation energies derived from batch experiments is problematic, as pointed out by Rytter et al.²³ Perhaps more appropriate is a comparison to computed results for the isolated elementary reaction. Computational predictions of the activation energies with DFT, as well as ab initio methods, give for biscyclopentadienylzirconocenium catalysts, or close analogues, values of $E_{\text{a,prop}}$ in the range of 2.8–6.4 kcal/mol.^{37,38} DFT calculations predict an activation barrier for associative chain transfer, predicted to be the preferred mechanism, $E_{\text{a,trans}}$, around 5–10 kcal/mol,^{23,37,38} in acceptable agreement with the measurement in the present work. Although other groups had suggested β -hydride transfer to metal,³⁹ a dissociative chain-transfer mechanism, recent experimental work indicates clearly that biscyclopentadienylzirconocenium systems operate predominantly by a β -hydride transfer to monomer.⁴⁰ More

important for the present topic, however, is the result for chain walking. The origin of branches in polyethylene has been attributed to several possible mechanisms. Reincorporation of vinyl-terminated macromonomers produced by a prior chain transfer, proposed for long-chain branching,¹⁹ can be ruled out in the present experiment because the concentration of macromonomers at the time of quenching is too low. Chain walking, first reported by Fink for a nickel-based catalyst,⁴¹ was extensively characterized by Brookhart for nickel and palladium systems.⁴² The mechanism involves a 1,2-elimination, followed by a 2,1-insertion, which suggests a close relationship to chain-transfer mechanisms. In analogy to chain transfer, chain walking could proceed by either β -hydride transfer to metal or β -hydride transfer to monomer, in principle. The reversible transfer-to-metal mechanism is established for chain walking in the late-transition-metal catalysts,⁴² and it has been presumed for biscyclopentadienylzirconocenium alkyl complexes, for which a DFT calculation produced an activation energy of 10 kcal/mol.²³ Unfortunately, this is essentially indistinguishable energetically from β -hydride transfer to monomer, which if reversible for an alkylzirconocenium cation (with coordinated ethylene), would also give an activation energy around 10–12 kcal/mol for chain walking. Accordingly, these latter two mechanisms for branch formation in the MAO-activated, Cp_2ZrCl_2 -catalyzed polymerization of ethylene cannot yet be distinguished with confidence. A much more extensive study is under way to try to resolve the ambiguity.

Conclusions

Fourier transform ion mobility spectrometry distinguishes between linear and branched alkyl chains produced in DCC-quenched polymerizations. The method generates size-selected branch contents for the oligomers present in the early stages of polyethylene production. The size-selected branch contents can be analyzed in a minimalistic kinetic model which extracts Arrhenius activation energies from the oligomer distributions and branch contents. These activation parameters agree well with literature values, where available. Methodologically, ion mobility should help provide the kinetic parameters required for kinetic models that predict polymer microstructure and, hence, polymer properties as a function of catalyst and process conditions.

Acknowledgment. We acknowledge support from the ETH Zürich and the Swiss Nationalfonds.

Supporting Information Available: A short guide to the fitting of the rate constants, as well as the full citation for ref 6. This material is available free of charge via the Internet at <http://pubs.acs.org>.

JA065482E

- (37) Lohrenz, J. C. W.; Woo, T. K.; Ziegler, T. *J. Am. Chem. Soc.* **1995**, *117*, 12793.
 (38) Talarico, G.; Blok, A. N. J.; Woo, T. K.; Cavallo, L. *Organometallics* **2002**, *21*, 4939.
 (39) Chien, J. C. W.; Wang, B. P. *J. Polym. Sci., Part A: Polym. Chem.* **1990**, *28*, 15.

- (40) Thorshaug, K.; Rytter, E.; Ystenes, M. *Macromol. Rapid Commun.* **1997**, *18*, 715.
 (41) Mohring, V. M.; Fink, G. *Angew. Chem., Int. Ed. Engl.* **1985**, *24*, 1001.
 (42) Schubbe, R.; Angermund, K.; Fink, G.; Goddard, R. *Macromol. Chem. Phys.* **1995**, *196*, 467.
 (42) Shultz, L.; Brookhart, M. *Organometallics* **2001**, *20*, 3975. Shultz, L.; Tempel, D. J.; Brookhart, M. *J. Am. Chem. Soc.* **2001**, *123*, 11539.